Computation of High-Speed Plasma Flows in the Conditions of Thermochemical Non-Equilibrium

Computation of High-Speed Plasma Flows in the Conditions of Thermochemical Non-Equilibrium

A M Molchanov

Moscow Aviation Institute (National Research University) ,
Russia, 125993 Moscow, Volokolamskoe shosse, 4

Alexmol_2010@mail.ru

Abstract. A numerical method is proposed for computing an ionized high-speed flow in the conditions of thermal and chemical nonequilibrium, taking into account the interaction of a moving electrically conductive continuous medium with an electromagnetic field. These flows are described by a fully coupled system of equations, which includes the equations of continuity, momentum, total energy, rotational energy, vibrational energy, electron energy, and mass conservation of chemical components. Electrical conductivity is determined using the kinetic theory. A special explicit-implicit scheme with alternation in half steps in time was proposed for numerical solution of rigid equations of chemical components and energy modes. That made it possible to solve a completely coupled system of equations with a large number of components and modes quickly and effectively. The developed method was used for numerical simulation of the physic process of interaction of a magnetic field with an ionized flow. The results of computations preformed by the proposed method are in satisfactory agreement with experimental data and computation results of other authors.

1. Introduction

As well known, an electromagnetic field affects an ionized gas flow. Many scientific papers are devoted to the study of this process (see, for example, [1,2]). Most of them, as a rule, use an assumption of chemical equilibrium of an ionized gas mixture and also an assumption that all energy modes of gas molecules are in thermal equilibrium, i.e. a flow is described by a single temperature.

However, real high-speed gas flows, especially at high altitudes, are characterized by significant chemical and thermal nonequilibrium [3].

The purpose of this work is to obtain the most complete mathematical model that describes a flow of an ionized high-speed gas mixture, taking into account the interaction of a moving electrically conductive continuous medium with an electromagnetic field. Special attention is paid to the calculation of electrical conductivity of such gas mixture based on the analysis of collision integrals of molecules and thermal motion of electrons.

2. Mathematical model

2.1. Governing equations

The equations of nonequilibrium flow within an imposed magnetic field include the equations of continuity, momentum, total energy, rotational energy, vibrational energy, electron energy and mass conservation of chemical components [3].

The sources that take into account electromagnetic forces are introduced in the equations of momentum and energy:

$$\mathbf{S}_{\mathrm{u}} = \mathbf{j}\times\mathbf{B}, \quad S_{\mathrm{E}} = \mathbf{j}\bullet\mathbf{E} \ , \tag{1}$$

where $\mathbf{B}$ is magnetic field strength; $\mathbf{j}$ is current density; $\mathbf{E}$ - is electric field strength.

The equations for rotational energy, vibrational energy, electron energy are as follows:

$$\frac{\partial}{\partial t}\left(\rho E_{\mathrm{R}}\right)+\nabla\bullet\left(\rho E_{\mathrm{R}}\mathbf{V}\right)=\rho\dot{E}_{\mathrm{R}}-\nabla\bullet\mathbf{q}_{R} \tag{2}$$

$$\frac{\partial}{\partial t}\left(\rho E_{\mathrm{V},m}\right)+\nabla\bullet\left(\rho E_{\mathrm{V},m}\mathbf{V}\right)=\rho\dot{E}_{\mathrm{V},m}-\nabla\bullet\mathbf{q}_{\mathrm{V},m}, \quad m=1,\ldots,N_{\mathrm{M}} \tag{3}$$

$$\frac{\partial}{\partial t}\left(\rho E_{\mathrm{e}}\right)+\nabla\bullet\left[\mathbf{V}\left(\rho E_{\mathrm{e}}+p_{\mathrm{e}}\right)\right]=\rho\dot{E}_{\mathrm{e}}-\nabla\bullet\mathbf{q}_{\mathrm{e}} \tag{4}$$

Here: ρ is the density of gas mixture; $\mathbf{V}$ is velocity vector; E_{R} is rotational energy per unit mass of the entire gas mixture; $E_{\mathrm{V},m}$ is the vibrational energy of the *m*-th mode per unit mass of the entire gas mixture; E_{e} is electron energy per unit mass of the entire gas mixture; $\mathbf{q},\mathbf{q}_{\mathrm{R}},\mathbf{q}_{\mathrm{V},m},\mathbf{q}_{\mathrm{e}}$ are density of heat fluxes: total energy, rotational energy, vibrational energy and energy of electrons, respectively; $\dot{E}_{\mathrm{R}},\dot{E}_{\mathrm{V},m},\dot{E}_{\mathrm{e}}$ are the sources in the energy equations associated with energy transitions; p_{e} is the electron pressure; N_{M} is the number of vibrational modes.

The following assumption is used: The magnetic Reynolds number is considered to be small, so the induced magnetic field is negligible.

Pressure is the sum of partial pressures:

$$p=\sum_{s\neq e}\rho_{s}\frac{R}{\mathrm{M}_{s}}T+p_{\mathrm{e}} \tag{5}$$

where M_{s} is the molar mass of species *s*; *R* is the universal gas constant.

The equations of state for electrons:

$$E_{\mathrm{e}}=C_{\mathrm{e}}\frac{3}{2}\frac{R}{\mathrm{M}_{\mathrm{e}}}T_{\mathrm{e}}, \quad p_{\mathrm{e}}=\rho_{\mathrm{e}}\frac{R}{\mathrm{M}_{\mathrm{e}}}T_{\mathrm{e}} \tag{6}$$

Here, the following assumptions were used: the electron dynamic pressure can be neglected and the excited electron states of molecules are negligible relative to the energies contained in other modes.

For the vibrational energy, we used an approach based on the model of a harmonic oscillator, according to which the average number of the *m*-th vibrational quanta α_{m} per one molecule is determined by the formula

$$\alpha_{m}=r_{m}\frac{1}{\exp\left(\theta_{m}/T_{\mathrm{V},m}\right)-1} \tag{7}$$

where θ_{m} is a characteristic vibrational temperature of the *m*-th vibrational mode; $T_{\mathrm{V},m}$ is appropriate vibrational temperature; r_{m} is the degree of degeneracy of the *m*-th mode of the molecule.

The specific (per unit mass of the component to which this mode belongs) vibrational energy of the *m*-th vibrational mode $e_{\mathrm{V},m}$ is related to α_{m} as following:

$$e_{\mathrm{V},m} = \frac{R\theta_m}{\mathrm{M}_{s(m)}}\alpha_m = \frac{r_m\theta_m\left(R/\mathrm{M}_{s(m)}\right)}{\exp\left(\theta_m/T_{\mathrm{V},m}\right)-1} \tag{8}$$

where $\mathrm{M}_{s(m)}$ is the molar mass of the species *s* to which the *m*-th vibrational mode belongs.

Heat fluxes in the equations (2)-(4) are determined by the formulas:

$$\mathbf{q}_{\mathrm{R}} = -\frac{\mu}{\mathrm{Pr}}\nabla E_{\mathrm{R}}, \quad \mathbf{q}_{\mathrm{V},m} = -\frac{\mu}{\mathrm{Pr}}\nabla E_{\mathrm{V},m}, \quad \mathbf{q}_{\mathrm{e}} = -\frac{\mu}{\mathrm{Pr}}\nabla h_{\mathrm{e}} \tag{9}$$

where h_{e} is the enthalpy of electrons

$$h_{\mathrm{e}} = E_{\mathrm{e}} + \frac{p_{\mathrm{e}}}{\rho} \tag{10}$$

When deriving the formulas (9), we used the assumption of similarity of heat transfer and diffusion, i.e. the equality of Schmidt and Prandtl numbers (Sc=Pr). The technique described in detail in [4] was used to calculate the coefficient of viscosity.

2.2. Energy Exchange Mechanisms

The source in the electron energy equation is

$$\rho\dot{E}_{\mathrm{e}} = Q_{\mathrm{T\text{-}e}} - \sum_m Q_{\mathrm{e\text{-}V},m} + \dot{w}_{\mathrm{e}}e_{\mathrm{e}} \tag{11}$$

where $e_{\mathrm{e}} = E_{\mathrm{e}}/C_{\mathrm{e}} = \frac{3}{2}\frac{R}{\mathrm{M}_{\mathrm{e}}}T_{\mathrm{e}}$; $Q_{\mathrm{T\text{-}e}}$ is translation-electron (T-e) energy transfer rate; $Q_{\mathrm{e\text{-}V},m}$ is electron-vibration energy transfer rate.

The source in the equation of the m-th vibrational energy is

$$\rho\dot{E}_{\mathrm{V},m} = Q_{\mathrm{T\text{-}V},m} + Q_{\mathrm{V\text{-}V},m} + Q_{\mathrm{e\text{-}V},m} - Q_{\mathrm{Rad\text{-}V},m} + \dot{w}_{s(m)}e_{\mathrm{V},m}\ , \tag{12}$$

where $Q_{\mathrm{T\text{-}V},m}$ is translation-vibration (T-V) energy transfer rate; $Q_{\mathrm{V\text{-}V},m}$ is vibrational-vibrational (V-V) energy transfer rate.

The source in the rotational energy equation is

$$\rho\dot{E}_{\mathrm{R}} = Q_{\mathrm{T\text{-}R}} + \sum_{s=1}^{N\mathrm{c}}\dot{w}_s e_{\mathrm{R},s}\ , \tag{13}$$

$Q_{\mathrm{T\text{-}R}}$ - is translational-rotational (T-R) energy transfer rate; $e_{\mathrm{R},s} = c_{\mathrm{v,R},s}T_{\mathrm{R}}$. It is assumed that the exchange of rotational energy with vibrational and electron energy can be neglected.

2.2.1. Translational-electron transfer rate

For the T-e energy transfer rate the formula of Lee was used [5]:

$$Q_{\mathrm{T\text{-}e}} = 3R\rho_{\mathrm{e}}\left(T - T_{\mathrm{e}}\right)\sqrt{\frac{8RT_{\mathrm{e}}}{\pi\mathrm{M}_{\mathrm{e}}}}\sum_{r\neq\mathrm{e}}\sigma_{\mathrm{e}r}\frac{\rho_r N_{\mathrm{A}}}{\mathrm{M}_r^{\,2}}\ , \tag{14}$$

where σ_{er} - are cross sections of electron collisions with heavy particles; N_{A} is Avogadro number.

The collision cross sections of electrons with neutral particles were calculated on the basis of the recommendations of Yukikazu Itikawa [6].

For the case of electron-ion interactions, the effective Coulomb cross section is given by [5]:

$$\sigma_{\mathrm{e,ions}} = \frac{8\pi}{27}\left(\frac{\lambda_{\mathrm{D}}}{T^*}\right)^2\ln\left(1+9T^{*2}\right),\ cm^2 \tag{15}$$

where Debye length is

$$\lambda_{\mathrm{D}} = \sqrt{\frac{k_{\mathrm{B,CGS}} T_{\mathrm{e}}}{4\pi n_{\mathrm{e,CGS}} q_{\mathrm{CGS}}^2}} \quad - \tag{16}$$

$$T^{*2} = \frac{{\lambda_{\mathrm{D}}}^2}{q_{\mathrm{CGS}}^4 / \left(k_{\mathrm{B,CGS}} T_{\mathrm{e}}\right)^2} = \frac{\left(k_{\mathrm{B,CGS}} T_{\mathrm{e}}\right)^3}{4\pi N_{\mathrm{e,CGS}} q_{\mathrm{CGS}}^6} \ , \tag{17}$$

$k_{\mathrm{B,CGS}}$ is the Boltzmann constant in CGS units, q_{CGS} is the electron charge in CGS units and $N_{\mathrm{e,CGS}}$ is the electron number density also in CGS units.

2.2.2. Electron-vibrational energy transfer rate

There is a significant exchange between the electron energy and the vibrational energy of molecular nitrogen. The exchange of the electron energy with the vibrational energy of other molecules is negligible. For the exchange of energy between the energy of electrons and the vibrational mode of nitrogen, the Landau-Teller formula is used:

$$Q_{\mathrm{e\text{-}V},m} = \rho_{s(m)} \frac{\mathrm{M}_{s(m)}}{\mathrm{M}_{\mathrm{e}}} \frac{e_{\mathrm{V},m}^{*}\left(T_e\right) - e_{\mathrm{V},m}}{\tau_{em}}, \quad for\ s(m) = \mathrm{N}_2 \tag{18}$$

where the relaxation time τ_{em} is a function of electron temperature and pressure derived by Lee [7].

2.2.3. The translational-rotational energy transfer rate

For the T-R energy transfer rate, the Landau-Teller formula was used:

$$Q_{\mathrm{T\text{-}R}} = \rho \frac{{E_{\mathrm{R}}}^{*}\left(T\right) - E_{\mathrm{R}}}{\tau_{\mathrm{R}}} \ , \tag{19}$$

where ${E_{\mathrm{R}}}^{*}\left(T\right) = T \sum_{s \neq e}^{Nc} C_s c_{\mathrm{v,R},s}$ is equilibrium rotational energy; τ_{R} is rotational relaxation time, for which the following formula is used [8]

$$\tau_{\mathrm{R}} = 5 \frac{\overline{\lambda}}{\overline{c}} \tag{20}$$

$\overline{c}$ is an average speed of molecules; $\overline{\lambda}$ is an average free path length of molecules.

2.2.4. Translational-vibrational energy transfer rate

The Landau-Teller model is used:

$$Q_{\mathrm{T\text{-}V},m} = \rho_{s(m)} \frac{e_{\mathrm{V},m}^{*}\left(T\right) - e_{\mathrm{V},m}}{\tau_m} \ , \tag{21}$$

where $e_{\mathrm{V},m}^{*}\left(T\right)$ is the equilibrium vibrational energy of the *m*-th mode. The relaxation time is calculated by the formula

$$\tau_m = \left(\sum_r X_r / \tau_{m,r} \right)^{-1} \sum_r X_r \ , \tag{22}$$

where X_r is mole fraction of species *r*. To calculate the times $\tau_{m,r}$, the formulas from [9-11] were used.

2.2.5. Vibrational-vibrational energy transfer rate

The general form of the V-V process is

$$\mathrm{A}^{*} + \mathrm{B} \rightleftarrows \mathrm{A} + \mathrm{B}^{*} \tag{23}$$

where A* is a vibrationally excited state of molecule A.
The following formulas are valid [9]:

$$\frac{d\alpha_{\mathrm{A}}}{dt}\Big|_{\text{V-V}} = \frac{X_{\mathrm{B}}}{\tau_{\mathrm{AB}}}\left[\left(1+\alpha_{\mathrm{A}}\right)\alpha_{\mathrm{B}}\exp\left(\frac{\theta_{\mathrm{B}}-\theta_{\mathrm{A}}}{T}\right)-\left(1+\alpha_{\mathrm{B}}\right)\alpha_{\mathrm{A}}\right] \tag{24}$$

$$\frac{d\alpha_{\mathrm{B}}}{dt}\Big|_{\text{V-V}} = \frac{X_{\mathrm{A}}}{\tau_{\mathrm{AB}}}\left[\left(1+\alpha_{\mathrm{B}}\right)\alpha_{\mathrm{A}}-\left(1+\alpha_{\mathrm{A}}\right)\alpha_{\mathrm{B}}\frac{\exp\left(\theta_{\mathrm{B}}/T\right)}{\exp\left[\theta_{\mathrm{A}}/T\right]}\right] \tag{25}$$

The total rate of formation of quanta of the *m*-th mode $\dot{\alpha}_{\text{V-V},m}$ consists of all the V-V processes occurring with this mode. There is a following relation between the rate of energy transfer and the change in the number of quanta $\dot{\alpha}_{\text{V-V},m}$:

$$Q_{\text{V-V},m} = \rho_{s(m)}\theta_m\frac{R}{\mathrm{M}_{s(m)}}\dot{\alpha}_{\text{V-V},m} \tag{26}$$

To calculate the relaxation times τ_{AB}, refer to the formulas from [9-11].

2.3. Electromagnetic field
According to Ohm's law, the current density is determined by the formula:

$$\mathbf{j} = \sigma_{\mathrm{e}}\left(\mathbf{E}+\mathbf{V}\times\mathbf{B}\right)$$

This form of equation neglects the Hall current for simplicity.
Electrical conductivity σ_{e} is determined using the kinetic theory. The formula Yos [12] is used:

$$\sigma_{\mathrm{e}} = \frac{{q_{\mathrm{e}}}^2 X_{\mathrm{e}}}{k_{\mathrm{B}}T_{\mathrm{e}}}\left(\sum_{j\neq\mathrm{e}}^{Nc} X_j{\Delta_{\mathrm{e}j}}^{(1)}\right)^{-1} = \frac{{q_{\mathrm{e}}}^2 N_{\mathrm{e}}}{k_{\mathrm{B}}T_{\mathrm{e}}}\left(\sum_{j\neq\mathrm{e}}^{Nc}{\Delta_{\mathrm{e}j}}^{(1)}N_j\right)^{-1}, \tag{27}$$

where

$${\Delta_{\mathrm{e}j}}^{(1)} = \frac{8}{3}\left[\frac{2\mathrm{M_e}\mathrm{M}_j}{\pi RT_{\mathrm{e}}\left(\mathrm{M}_e+\mathrm{M}_j\right)}\right]^{1/2} 10^{-20}\pi{\Omega_{\mathrm{e}j}}^{(1,1)}\left(T_{\mathrm{e}}\right) \tag{28}$$

Here: $\pi{\Omega_{ij}}^{(1,1)}$ is diffusion collision integral; k_{B} is the Boltzmann constant; q_{e} is elementary charge; X_{e} is electron mole fraction; T_{e} is electron temperature; N_{e} is electron number density.
The constant 10^{-20} converts square Angstroms into square meters, which is a standard unit for collision integrals. The recommended values of Collision Integrals for the pairs N_2-e, O_2-e, N-e, O-e, NO-e, C-e, CO_2-e, CO-e, CN-e, C_2-e are taken from Wright et al. [13].

2.4. Chemical kinetics
The following system of chemical reactions is used for the calculation of high-enthalpy air flows

$\mathrm{N_2+M \rightleftarrows 2N+M}$ $\qquad$ $\mathrm{N+O \rightleftarrows NO^+ + e^-}$
$\mathrm{O_2+M \rightleftarrows 2O+M}$ $\qquad$ $\mathrm{N+e^- \rightleftarrows N^+ + e^- + e^-}$
$\mathrm{NO+M \rightleftarrows N+O+M}$ $\qquad$ $\mathrm{O+e^- \rightleftarrows O^+ + e^- + e^-}$
$\mathrm{N_2+O \rightleftarrows NO+N}$ $\qquad$ $\mathrm{N+N \rightleftarrows {N_2}^+ + e^-}$
$\mathrm{NO+O \rightleftarrows N+O_2}$ $\qquad$ $\mathrm{O+O \rightleftarrows {O_2}^+ + e^-}$

In some problems, the reactions involving H_2O, H_2, OH, H, CO_2, CO, C were added (see [3]), as well as the reaction of cesium ionization

$$\mathrm{Cs+e^- \rightleftarrows Cs^+ + e^- + e^-}$$

The details of determining reaction rates and component formation rates, as a result of chemical reactions, can be found in [3].

3. Numerical method

The vector form of the governing equations in the Cartesian coordinate system is

$$\frac{\partial \mathbf{U}}{\partial t} + \mathrm{K}\left(\mathbf{U}\right) = \mathbf{S}\left(\mathbf{U}\right) \tag{29}$$

where

$$\mathbf{U} = \left(\rho, \rho u, \rho v, \rho w, \rho E, \rho E_{\mathrm{R}}, \rho E_{\mathrm{V},1}, ..., \rho E_{\mathrm{V},N_m}, \rho E_{\mathrm{e}}, \rho C_1, ..., \rho C_{Nc-1}\right)^T , \tag{30}$$

u, v, w are velocity components in the Cartesian coordinate system; E - total energy; $\mathrm{K}\left(\mathbf{U}\right)$ is the vector representation of inviscid and viscous fluxes (see [3]); $\mathbf{S}\left(\mathbf{U}\right)$ is the source vector

$$\mathbf{S}\left(\mathbf{U}\right) = \left(0, f_x, f_y, f_z, s_{\mathrm{E}}, \rho \dot{E}_{\mathrm{R}}, \rho \dot{E}_{\mathrm{V},1}, ..., \rho \dot{E}_{\mathrm{V},N_{\mathrm{M}}}, \rho \dot{E}_{\mathrm{e}}, \dot{w}_1, ..., \dot{w}_{N_{\mathrm{C}}-1}\right)^T , \tag{31}$$

Here: $f_x = j_y B_z - j_z B_y$, $f_y = j_z B_x - j_x B_z$, $f_z = j_x B_y - j_y B_x$, $s_E = j_x E_x + j_x E_x + j_x E_x$

$j_x = \sigma_{\mathrm{e}}\left(E_x + V_y B_z - V_z B_y\right)$, $j_y = \sigma_{\mathrm{e}}\left(E_y + V_z B_x - V_x B_z\right)$, $j_z = \sigma_{\mathrm{e}}\left(E_z + V_x B_y - V_y B_x\right)$

The most efficient way for solving system (29) is a fully coupled numerical method, i.e. a simultaneous solution of the entire system. In addition, it is preferable to use implicit methods in order to avoid strict limitations on the time step in terms of stability.

In terms of sources, the system (29) is stiff. This applies to the electromagnetic interaction in the equations of momentum and total energy, and to energy transitions in the equations of rotational, vibrational and electronic energies, and chemical sources of species. Direct numerical solution of these equations requires a very small time step and huge computer resources.

To solve this problem, we propose the following explicit-implicit scheme with alternation at half steps. At each time step $\Delta t = t^{n+1} - t^n$, a step is divided into two half-steps $\Delta t / 2$, and the system is solved in two stages:

First half step:
$$\frac{\Delta \tilde{\mathbf{U}}_{i,j,k}}{\Delta t / 2} + \mathrm{K}\left(\mathbf{U}^n_{i,j,k}\right) = \mathbf{S}\left(\tilde{\mathbf{U}}_{i,j,k}\right) \tag{32}$$

Second half-step:
$$\frac{\delta \tilde{\mathbf{U}}_{i,j,k}}{\Delta t / 2} + \mathrm{K}\left(\mathbf{U}^{n+1}_{i,j,k}\right) = \mathbf{S}\left(\tilde{\mathbf{U}}_{i,j,k}\right) \tag{33}$$

$$\Delta \tilde{\mathbf{U}}_{i,j,\mathrm{k}} = \tilde{\mathbf{U}}_{i,j,\mathrm{k}} - \mathbf{U}^n_{i,j,\mathrm{k}}, \quad \delta \tilde{\mathbf{U}}_{i,j,\mathrm{k}} = \mathbf{U}^{n+1}_{i,j,\mathrm{k}} - \tilde{\mathbf{U}}_{i,j,\mathrm{k}} \quad \Rightarrow \quad \delta \mathbf{U}^{n+1}_{i,j,\mathrm{k}} = \delta \tilde{\mathbf{U}}_{i,j,\mathrm{k}} + \Delta \tilde{\mathbf{U}}_{i,j,\mathrm{k}} \tag{34}$$

Here: $\mathbf{U}^n_{i,j,\mathrm{k}}$ is the value of the vector in the grid node (*i*,*j*,*k*) at time t^n; $\mathrm{K}\left(\mathbf{U}^n_{i,j,k}\right)$ is a finite volume approximation of viscous and inviscid fluxes.

With this approach, both physical processes are taken into account at each stage, but their explicit and implicit presentation alternates.

The equation (32) is solved as a system of ordinary differential equations:

$$\left[\mathbf{I} - 0.5\Delta t\left(\frac{\partial \mathbf{S}}{\partial \mathbf{U}}\right)^n_{i,j,k}\right]\left(2\Delta \tilde{\mathbf{U}}_{i,j,k}\right) = \Delta t \mathbf{S}\left(\mathbf{U}^n_{i,j,k}\right) - \Delta t \mathrm{K}\left(\mathbf{U}^n_{i,j,k}\right) \tag{35}$$

Its solution is not a big problem.

At the second stage, the source is presented in an explicit form, and the solution of the system (33) is not fundamentally different from the solution of a vector equation by a zero source. Implicit numerical methods for solving such a system are described in many papers, in particular [14, 3].

With an implicit representation of viscous and inviscid fluxes at each time step in each node of the grid, there is a need for multiple inversions of Jacobian matrices, as well as for carrying out multiplication operations of such matrices.

In that case, all these matrices, and, most importantly, matrices that appear in intermediate calculations, have a general block form:

$$\mathbf{A} = \begin{pmatrix} \mathbf{A}_{11} & \mathbf{0} \\ \mathbf{A}_{21} & \mathbf{D} \end{pmatrix} \tag{36}$$

where matrix blocks have the following sizes: $\mathbf{A}_{11}$ - 5x5; $\mathbf{A}_{21}$ - N_ax5; $\mathbf{D}$ is a diagonal matrix of size N_a. Here, N_a is a number of additional equations; $N_a+5 = N_{eq}$ is a total number of equations. The matrix $\mathbf{A}_{11}$ refers to the basic Navier-Stokes equations (equations of continuity, momentum and energy).

The main advantages of the matrix of the form (36) are: 1) its inversion is reduced to a single inversion of matrix $\mathbf{A}_{11}$ and trivial matrix multiplication operations; 2) any necessary operations with such a matrix do not change its form, i.e. the block $\mathbf{A}_{12}$ remains zero, and the $\mathbf{A}_{22}$ block remains a diagonal matrix. So, even a significant increase in the number of additional equations does not lead to a significant increase in the cost of computer resources.

Thus, a fully coupled numerical scheme for solving the basic system of equations, which is unconditionally stable, is obtained. Its solution does not impose any strict restrictions on the time step and does not require the inversion of large matrices.

4. Results

4.1. Ram-C Flight Experiment

The most important factor influencing the interaction of a moving electrically conductive continuous medium with an electromagnetic field is concentration of electrons. During the 1960's a series of flight experiments [15] were made, during which electron number densities were measured using microwave reflectometers. The vehicle was a sphere-cone body, with a 9º cone half angle and a length of 1.295m. The calculations were carried out for altitudes of 72, 81, 85 km.

The present case was chosen as a test case to check the results using non-equilibrium chemistry model 1 using 7 species, N_2, O_2, NO, NO, N, O and e^-. Cesium was included but played no part because the initial mass concentrations were set to zero.

Peak electron densities, within the shock layer around the body, are compared in figure 1. The comparison between experiment shown by the symbols and computation is fairly good. Figure 2 shows the change in the translational and electron temperatures along the stagnation streamline for an altitude of 81 km.

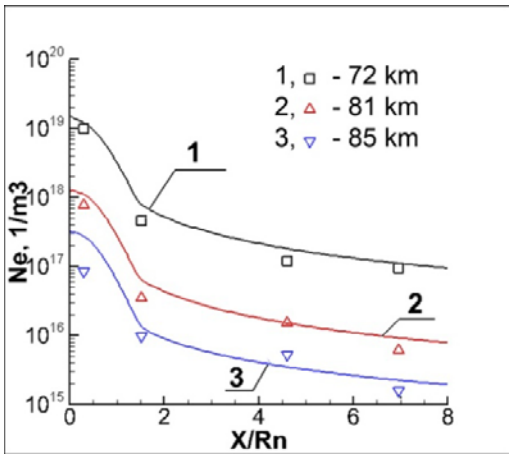

Figure 1. Peak electron number density. Lines - computation; Symbols - experiment [15].

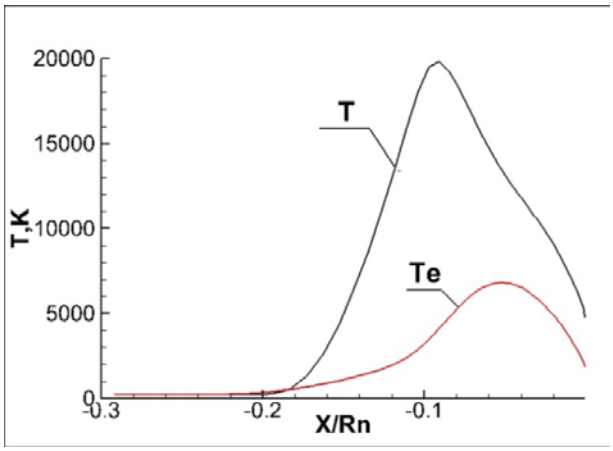

Figure 2. Temperatures on stagnation streamline. 81 km.

Figure 3 shows the electrical conductivity of the gas mixture along the stagnation streamline for an altitude of 81 km using various methods for calculating it.

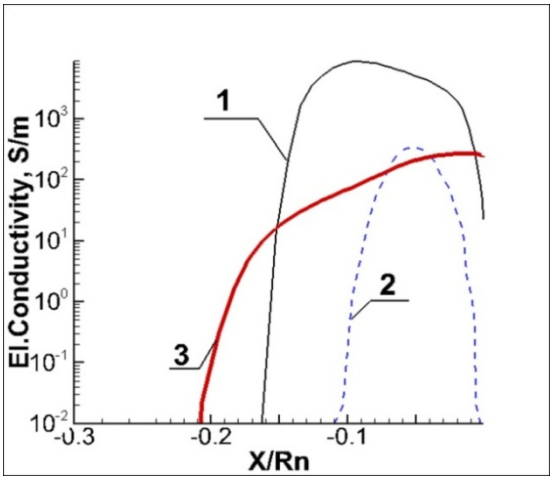

Figure 3. The electrical conductivity of the gas mixture along the stagnation streamline for an altitude of 81 km using various methods of its calculation.
1 - calculation using the assumption of thermochemical equilibrium of air; the translational temperature is used as a determinative;
2 - calculation using the assumption of thermochemical equilibrium of air; electron temperature is used as a determining factor;
3 - calculation of thermo-chemically non-equilibrium.

It is obvious that thermo-chemical nonequilibrium significantly affects the conductive properties of the gas mixture.

4.2. Ziemer Experiment

In 1959 Ziemer [16] reported the results of an experimental investigation in magneto-aerodynamics. He placed a hemi-spherically nosed cylinder of diameter 0.02m and made of Pyrex glass within an electromagnetic shock tube. A blast wave moved at Mach 21.5 into stationary air, at temperature 273K and pressure 9.33N/m2, past the model, producing a hypervelocity flow of ionized air.

We chose the conditions to be within the experimental conditions of Ziemer's [16]. The method described in chapter 3 was used for the calculations.

The magnetic field distribution in the free stream is that of a dipole at the origin (i.e., at the center of curvature of the nose radius r_n). This distribution is mathematically expressed by

$$\mathbf{B} = B_0 \frac{r_n^3}{r^3} \cos\theta \, \mathbf{e}_r + B_0 \frac{r_n^3}{2r^3} \sin\theta \, \mathbf{e}_\theta \tag{37}$$

where $\mathbf{e}_r$ and $\mathbf{e}_\theta$ are unit vectors in the radial direction relative to the center of the cylinder and the θ direction with θ measured from the axis. A magnetic interaction parameter: $Q^* = \sigma_e B_o^{\,2} r_n / \left(\rho_\infty u_\infty\right)$ was used to estimate the intensity of the electromagnetic effect. The free flow conditions for the present flow modeling are shown in table 1 (the concentrations of the components are given in mole fractions). The conductivity was taken average behind shock wave.

Table 1. Free Stream Conditions

Velocity (ms^{-1})	Pressure (Pa)	Temperature (K)	O	O_2	NO	N	NO^+	N_2
5690	3013	9813	0.05	0.1715	0.016	0.0422	0.00025	0.72018

The pressure contours for the flow about the model are shown above in figures 4 and 5 with and without the dipole magnetic field. When the magnetic field was turned on, the standoff distance of the bow shock wave from the model nose increased from 0.0029m to 0.017m, a factor 5.9 times further.

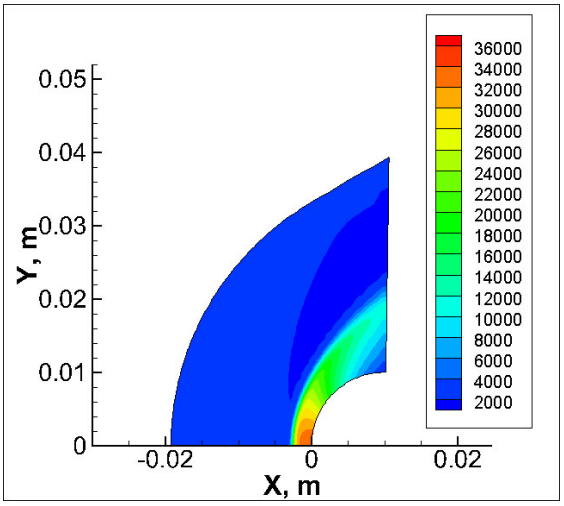

Figure 4. Pressure countours at Q*=0

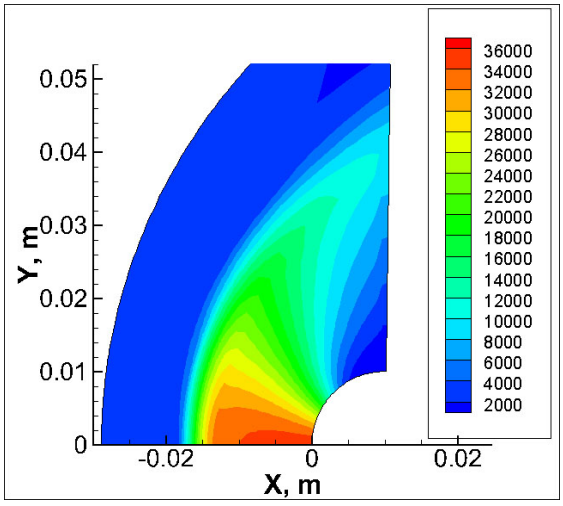

Figure 5. Pressure countours at Q*=55

The increase in shock standoff according to the interaction parameter is quantified and compared with experimental data in figure 6. The predictions of Bush's theory [1] are compared with the results of computations from [17] and these computations. It is shown that there is a very good match between the experiments and simulations. The shock standoff distance increased by a factor of up to 6.9 times when the magnetic field was turned on. Since the magnetic force tends to oppose flow across the magnetic field lines, the effect of the applied field is to slow the flow in regions where the local interaction parameter is larger.

Figure 7 shows the distribution of heat flux along the cylinder surface when calculating with and without the dipole magnetic field. It is obvious that the application of the electromagnetic field significantly reduces the heat flux into the wall.

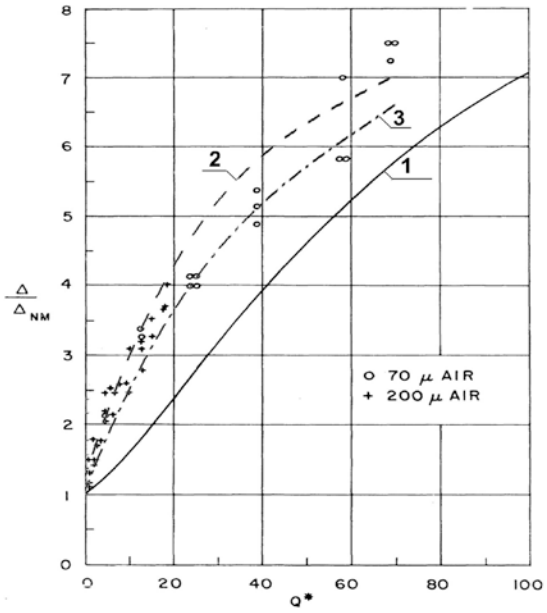

Figure 6. Comparison of shock standoff distances with experiments. 1 - calculation of Bush at thermochemical equilibrium [1]; 2 - calculation of Lee et all. [17]; 3 - calculation of this work; Symbols - experiments [16].

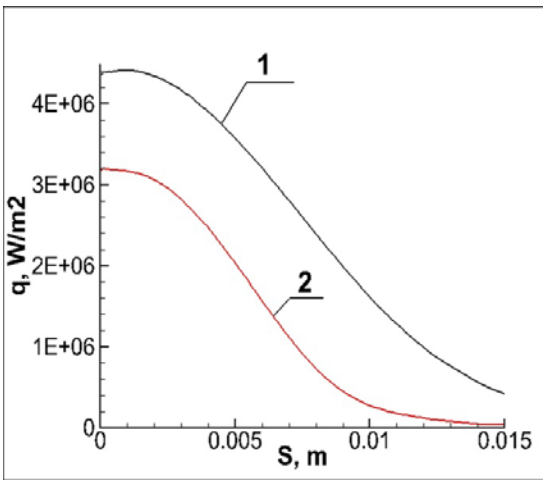

Figure 7. Comparison of surface heating-rate distribution:
1 - calculation at Q*=0;
2 - calculation at Q*=55.

5. Conclusions

The paper presents a numerical procedure for solving MFD problem including multi species, chemical reactions, rotational energy, vibrational energy and electron energy. A special explicit-implicit scheme with alternation in half steps in time was proposed for numerical solution of rigid equations of chemical components and energy modes, which made it possible to solve a completely coupled system of equations with a large number of components and modes quickly and effectively. Two different test cases were simulated using this numerical tool, showing an excellent match with published data and computations. In the first case, RAM-C flow case demonstrated the accuracy of the non-equilibrium flow solver module. In the second case, change in the shock standoff distance caused by applied magnetic fields is numerically computed and compared with Ziemer's experiments.

6. References

[1] Bush B 1958 *J. Aerosp. Sci.* **25** 685-90
[2] Poggic J and Gaitonde D 2002 *Phys. Fluids*. **14** 1720-31
[3] Molchanov A 2017 *Mathematical Modeling of Hypersonic Homogeneous and Heterogeneous Non-equilibrium Flows in the Presence of Complex Radiation-convective Heat Exchange* (Moscow: MAI) chapter 4 pp 44–51
[4] Scalabrin L 2007 *Numerical Simulation of Weakly Ionized Hypersonic Flow over Reentry Capsules* (Ann Arbor, Michigan: The University of Michigan) pp.21-25
[5] Lee J 1985 *Progress in Aeronautics and Astronautics: Thermal-Design of Aeroassisted Orbital Transfer Vehicles* vol 96, ed H F Nelson (New York: AIAA) pp 3-53
[6] Itikawa Y 2006 *J. Phys. Chem. Ref. Data* **35** 31-53
[7] Lee J 1986 *Progress in Aeronautics and Astronautics: Thermophysical Aspects of Re-entry Flows* vol 103, ed J N Moss and C D Scott (New York: AIAA) pp 197-224
[8] Gokcen T 1991 *Hypersonic Flows for Reentry Problems* (Berlin: Springer-Verlag)
[9] Losev S, Potapkin B, Macheret S and Chernyi G 2004 *Physical and Chemical Processes in Gas Dynamic* (Richmond, TX: AIAA)
[10] Blauer J and Nickerson G 1974 A Survey of Vibrational Relaxation Rate Data for Processes Important to CO2-N2-H2O Infrared Plume Radiation *AIAA Paper* 1974-536
[11] Ashratov E and Dubinskaya N 1977 *Investigation of nozzle flows with vibrational relaxation. Computational Methods and Programming* (Moscow: MGU) pp 96-115
[12] Yos J 1963 *Transport Properties of Nitrogen, Hydrogen, Oxygen, and Air to 30,000 K* (Wilmington: Ma Research and Advanced Development Div) pp 5-73
[13] Wright M, Bose D, Palmer G. and Levin E 2005 *AIAA J.* **43** 2558–64
[14] MacCormack R 2008 Flow Simulations within Strong Magnetic Fields *AIAA Paper* 2008-1070
[15] Granthan W 1970 *Flight results of 25,00 foot per second reentry experiment using microwave reflectometers to measure plasma electron density and standoff distance* (Hampton, VA: NASA TN D-6062) pp 1-92
[16] Ziemer R 1959 *ARS J.* **29** 642-7
[17] Lee J, Kim T and MacCormack R 2015 Simulation of Hypersonic Flow within Electromagnetic Fields for Heat Flux Mitigation *AIAA Paper* 2015-3503